ESC European Society of Cardiology

Cardiovascular Research (2018) **114**, 389–400
doi:10.1093/cvr/cvx163

Electrical coupling between ventricular myocytes and myofibroblasts in the infarcted mouse heart

Michael Rubart[1]*, Wen Tao[1], Xiao-Long Lu[1], Simon J. Conway[1], Sean P. Reuter[1], Shien-Fong Lin[2], and Mark H. Soonpaa[1,3]

[1]Wells Centre for Pediatric Research, Indiana University School of Medicine, 1044 West Walnut Street, Indianapolis, IN 46202, USA;[2]Institute of Biomedical Engineering, National Chiao Tung University, Hsinchu, Taiwan; and [3]Krannert Institute of Cardiology, Indiana University School of Medicine, Indianapolis, IN 46202, USA

Received 8 June 2016; revised 25 May 2017; editorial decision 9 August 2017; accepted 10 August 2017; online publish-ahead-of-print 1 September 2017

Time for primary review: 42 days

Aims Recent studies have demonstrated electrotonic coupling between scar tissue and the surrounding myocardium in cryoinjured hearts. However, the electrical dynamics occurring at the myocyte–nonmyocyte interface in the fibrotic heart remain undefined. Here, we sought to develop an assay to interrogate the nonmyocyte cell type contributing to heterocellular coupling and to characterize, on a cellular scale, its voltage response in the infarct border zone of living hearts.

Methods and results We used two-photon laser scanning microscopy in conjunction with a voltage-sensitive dye to record transmembrane voltage changes simultaneously from cardiomyocytes and adjoined nonmyocytes in Langendorff-perfused mouse hearts with healing myocardial infarction. Transgenic mice with cardiomyocyte-restricted expression of a green fluorescent reporter protein underwent permanent coronary artery ligation and their hearts were subjected to voltage imaging 7–10 days later. Reporter-negative cells, i.e. nonmyocytes, in the infarct border zone exhibited depolarizing transients at a 1:1 coupling ratio with action potentials recorded simultaneously from adjacent, reporter-positive ventricular myocytes. The electrotonic responses in the nonmyocytes exhibited slower rates of de- and repolarization compared to the action potential waveform of juxtaposed myocytes. Voltage imaging in infarcted hearts expressing a fluorescent reporter specifically in myofibroblasts revealed that the latter were electrically coupled to border zone myocytes. Their voltage transient properties were indistinguishable from those of nonmyocytes in hearts with cardiomyocyte-restricted reporter expression. The density of connexin43 expression at myofibroblast–cardiomyocyte junctions was ~5% of that in the intercalated disc regions of paired ventricular myocytes in the remote, uninjured myocardium, whereas the ratio of connexin45 to connexin43 expression levels at heterocellular contacts was ~1%.

Conclusion Myofibroblasts contribute to the population of electrically coupled nonmyocytes in the infarct border zone. The slower kinetics of myofibroblast voltage responses may reflect low electrical conductivity across heterocellular junctions, in accordance with the paucity of connexin expression at myofibroblast-cardiomyocyte contacts.

Keywords Cardiac fibroblast • Electrical coupling • Two-photon fluorescence microscopy • Myocardial infarction • Periostin

1. Introduction

Fibrosis plays an important role in cardiac arrhythmias.[1] Myofibroblasts which are not normally present in the working myocardium but accumulate in large numbers in injured or aged hearts, critically contribute to fibrosis-related arrhythmogeneity. A number of *in vitro* and *in silico* studies have demonstrated that (myo)fibroblasts (which are electrically non-excitable cells) evoke arrhythmogenic electrotonic interactions with adjacent cardiomyocytes following establishment of heterocellular gap junctions.[2–5] Recent studies have provided functional evidence for the existence of electrical coupling between scar tissue and the surrounding myocardium in living injured hearts. Mahoney and co-workers observed reciprocal electrotonic conduction between the scar tissue and uninjured myocardium in the cryoinjured mouse heart through epicardial optical voltage mapping.[6] Using an identical injury model in conjunction with fluorescence measurements from small regions across the

* Corresponding author. Tel: +317 274 2007; fax: +317 278 9298, E-mail: mrubartv@iu.edu

epicardial surface, Quinn *et al.* observed cardiomyocyte action potential-like electrical activity at the scar border tissue in transgenic mice in which expression of a genetically encoded voltage sensor was targeted to non-myocytes, including myofibroblasts.[7] While these studies demonstrate the existence of heterocellular electrotonic coupling in the living injured heart, the techniques employed were not suitable to simultaneously interrogate, with cellular resolution, the voltage responses of nonmyocyte membranes and those of their juxtaposed cardiomyocyte membranes *in situ*. Such ability, however, could be crucial to understand open questions such as the extent of recruitment of nonmyocytes to the electrical syncytium of the fibrotically remodelled myocardium, electrical function and properties of single, coupled nonmyocytes *in situ*, and how coupled nonmyocytes respond to changes in the electrical activity of the adjoined cardiomyocytes. Here, we examined the utility of two-photon laser scanning microscopy (TPLSM) in conjunction with a fluorescent potentiometric dye to optically record, on a micron scale, transmembrane voltage changes from myocytes and single juxtaposed nonmyocytes simultaneously *in situ* within the infarct border zone of the Langendorff-perfused mouse heart.[8] To distinguish nonmyocytes from cardiomyocytes during vital TPLSM imaging, we utilized two independent, fluorescence-based reporter mouse models. Our results document the capability of the approach to not only co-register the electrical dynamics of single nonmyocytes and adjacent cardiomyocytes *in situ* but to also resolve differences in the kinetics between their respective voltage transients.

2. Methods

2.1 Coronary artery ligation

Animals were handled in accordance with the institutional guidelines and the investigation conforms to the Guide for the Care and Use of Laboratory Animals published by the US National Institutes of Health. Mice with cardiomyocyte- or myofibroblast-restricted expression of a green fluorescent reporter protein underwent coronary artery ligation to induce myocardial infarction injury.[9]

2.2 Immunofluorescence labelling

Tissues were processed for immunofluorescence labelling and confocal imaging as described previously.[10]

2.3 TPLSM of Langendorff-perfused mouse heart

Infarcted hearts were loaded with the potentiometric dye ANNINE-6plus and subjected to TPLSM voltage imaging as previously described.[8]

2.4 Statistics

In all cases, data distribution was tested using *Shapiro–Wilk's* normality test. The *t*-test or *Mann–Whitney Rank Sum* test was used to compare parameters between two experimental groups. *Kruskal–Wallis ANOVA* on ranks (followed by *Dunn's* test for multiple comparisons) was used to compare connexin densities. A P value of ≤ 0.05 was considered significant. Values are presented either as mean ± SEM, or median with interquartile range.

A detailed Methods section can be found in the Online Supplement.

3. Results

3.1 Nonmyocytes electrically couple to ventricular myocytes in the infarct border zone

We used TPLSM in conjunction with a fluorescent potentiometric dye for *in situ* optical recording of transmembrane voltage changes from myocytes and juxtaposed nonmyocytes simultaneously within the infarct border zone of the Langendorff-perfused mouse heart.[8] Myocardial infarction was induced by ligation of the left coronary artery in 3- to 4-month-old MHC-EGFP transgenic mice, typically resulting in the formation of large transmural scars (see Supplementary material online, *Figure S1*). Transgenic cardiomyocytes express EGFP both in their sarco- and nucleoplasm.[11] Immunofluorescence analyses of MHC-EGFP hearts at 7–10 days post ligation confirmed cardiomyocyte-restricted expression of the reporter transgene (see Supplementary material online, *Figure S2*), supporting its utility for discrimination of myocytes vs. nonmyocytes during vital imaging. For TPLSM imaging, MHC-EGFP hearts with 7- to 10-day-old infarcts were harvested, retrogradely perfused in Langendorff mode, and loaded with the voltage-sensitive fluorescent dye ANNINE-6plus. During imaging, hearts were perfused with Tyrode's solution supplemented with blebbistatin and ryanodine to uncouple contraction from excitation (and thereby eliminate motion artefacts during image acquisition). Voltage images were acquired from the lateral border zones which are characterized by the presence of strands of surviving cardiomyocytes separated by nonmyocyte clusters (see Supplementary material online, *Figure S1*).

A representative example of a frame-mode fluorescence image taken from the infarct border zone in a dye-loaded MHC-EGFP heart is shown in *Figure 1A*. EGFP-expressing ventricular myocytes can be readily identified by virtue of their green fluorescent sarcoplasm. ANNINE-6plus, which selectively stains surface membranes and emits predominately in the red range under the imaging conditions employed, labelled the sarcolemma of the cardiomyocytes, including their t-tubular components (see lower panel in *Figure 1A*). The dye also marked outer membranes of cells without detectable levels of green EGFP fluorescence in their cytoplasm, i.e. nonmyocytes, which were clustered between myocytes. The close proximity of myocytes and nonmyocytes enabled us to interrogate their electrical activities simultaneously, using the high temporal resolution afforded by the line-scan acquisition mode of the imaging system. Accordingly, a line traversing myocyte and juxtaposed nonmyocyte membranes (dotted line in *Figure 1A*) was repetitively scanned to generate line scan fluorescence $F(x, t)$ images as shown in *Figure 1B*. Data was acquired while the heart was electrically paced at a remote site at a frequency of 3 Hz. The stacked line-scan images revealed periodic decreases in ANNINE-6plus fluorescence, reflecting depolarizing transients, in the myocyte membranes (left panel) occurring concomitantly with those in the juxtaposed nonmyocyte membranes (right panel), suggesting that they were entrained.

Averaged $\Delta F/F_0(t)$ traces were generated from the line-scan data (*Figure 1C*); the black trace represents the average in the myocyte (marked by the black bracket in *Figure 1A*), while the red trace is the average in the nonmyocyte marked by the red bracket. Fluctuations in transmembrane potential in the nonmyocyte occurred in phase with the action potentials in the juxtaposed myocytes in a 1:1 ratio, supporting the notion that the nonmyocytes were electrically coupled to ventricular myocytes. Superimposition of ensemble averages $\Delta F/F_0(t)$ (*Figure 1D and E*) revealed smaller peak $\Delta F/F_0$, as well as slower upstroke and recovery

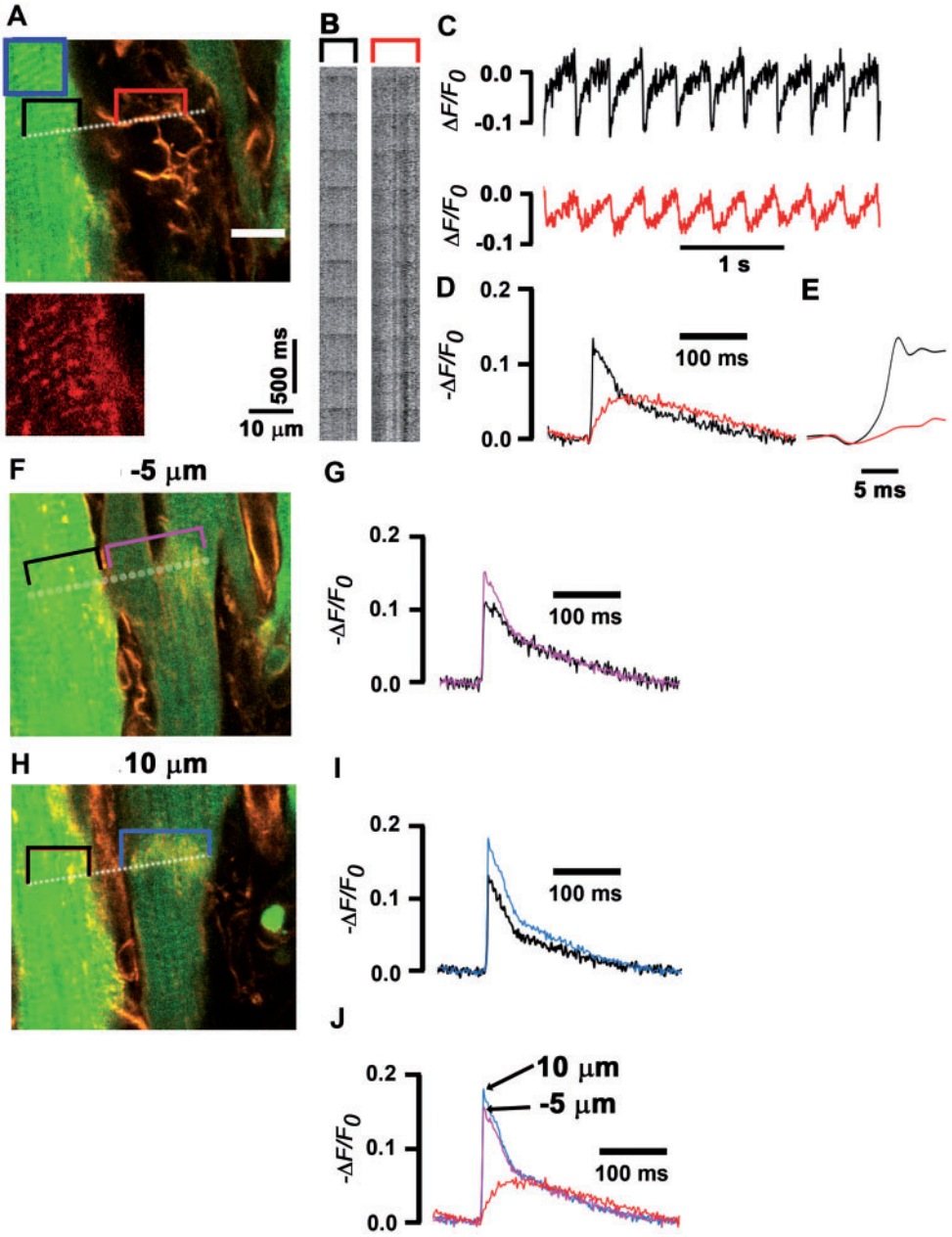

Figure 1 Entrainment of nonmyocyte membrane potential by the ventricular action potential in in the border zone of chronic myocardial infarction. *A*, *F*, and *H*, Series of frame-mode fluorescence images taken from the infarct border zone of an ANNINE-6plus—loaded MHC-EGFP heart 8 days following coronary artery ligation. EGFP marks cardiomyocytes. ANNINE-6plus selectively stains cell surface membranes and emits predominately in the red range under the conditions used here. Lower panel in *A* is magnified view of the red signal in the boxed region (blue) in the upper panel. The images were being acquired while the heart was electrically paced at a frequency of 3 Hz. Numbers in μm denote *z*-axis distances of the focal plane from that in panel A. White scale bar 10 μm. *B*, Line-scan fluorescence $F(x, t)$ images for the segments of the scanning lines marked by correspondingly coloured brackets in panel *A*. Images were acquired by repetitively scanning along the dotted line. Each $F(x, t)$ image was composed of 8 000 line-scans. Periodic decreases in ANNINE-6plus fluorescence reflect depolarizing voltage transients in response to electrical pacing at a remote site. To reduce staining inhomogeneities, the fluorescence intensity of each pixel was normalized to $F_o(x, t)$, the average F at the x^{th} pixel over a 20-ms time period preceding the voltage transients. The images were low-pass filtered (filter half-widths 0.42 μm and 4 ms), and the contrast increased. *C*, Line averages $\Delta F/F_o(t)$ for the colour-coded segments in A. Traces are excerpts from line-scan recordings comprising 42 consecutive voltage transients and were filtered by a 5-point moving average. *D*, *G*, and *I*, Ensemble averages $-\Delta F/F_o(t)$ over the segments of the scanning lines marked by colour-coded brackets in the corresponding panels in *A*, *F*, and *H*. Each trace represents the average of 42 consecutive cycles. *E*, Upstrokes of myocyte and nonmyocyte $\Delta F/F_o$ transients in *D* on an expanded time scale. *J*, Superimposition of the ensemble averages $-\Delta F/F_o(t)$ for the nonmyocyte (red segment in panel *A*) and the two apposed myocytes (purple and blue segments, respectively, in panel *F* and *H*).

kinetics, of the $\Delta F/F_o(t)$ transient in the nonmyocyte compared with that in its juxtaposed myocyte. The membrane potential in the coupled nonmyocyte continued to increase beyond the time points of peak membrane depolarization in their respective adjacent myocytes, producing repolarization phase shifts between the two transients (*Figure 1D*).

Gradual decreases in axial resolution with increasing imaging depth in biological specimens in multiphoton fluorescence excitation microscopy[12] can give rise to the possibility that fluorescence signals obtained from nonmyocytes were actually arising from over- and/or underlying border zone cardiomyocytes (signal bleed-through), feigning heterocellular coupling. If this were the case, we would expect action potential-related changes in ANNINE-6plus fluorescence recorded in nonmyocytes to be scaled replicas of the fluorescence changes detected in radially apposed myocytes. Accordingly, we compared the kinetics of action potential-related fluorescence changes recorded from nonmyocytes with those of optical action potentials recorded from the nearest, radially apposed myocytes, as shown in *Figure 1F–I*. Imaging was performed by first scanning a line spanning an EGFP-positive ventricular myocyte and juxtaposed, EGFP-negative nonmyocytes (*Figure 1A*). The focal plane was then shifted -5 and +10 μm along the *z*-axis, and sequential $F(x, t)$ images were obtained along lines traversing portions of over- and underlying myocytes that apposed the nonmyocyte segments scanned in the first $F(x, t)$ image (*Figure 1F* and *H*, respectively). Superimposition of the ensemble averages $-\Delta F/F_o(t)$ from the nonmyocyte (red trace in *Figure 1D*) and those of its radially apposed cardiomyocytes (purple and blue traces in *Figure 1G* and *I*, respectively) revealed distinct differences in the time course of voltage changes between the two cell types (*Figure 1J*). Notably, the initial depolarization rose much more slowly in the nonmyocyte compared to either one of the bordering myocytes (the 10%–90% rise times were 39 ms in the nonmyocyte and 3 ms in either one of the axially apposed ventricular myocytes), supporting the notion that ANNINE-6plus fluorescence crossover was negligible. Collectively, these results support the notion that comparative analyses of $-\Delta F/F_o(t)$ kinetics profiles from nonmyocytes with those from their radially apposed cardiomyocytes enable elimination of signal crossover artefacts under the experimental conditions employed. As a consequence, $-\Delta F/F_o(t)$ recordings from nonmyocytes that exhibited time courses of initial depolarization indistinguishable from those of their under- or overlying myocytes, were excluded from the study (three out of a total of 41 $F(x, t)$ image series acquisitions distributed among 13 MHC-EGFP hearts).

Additional examples of heterocellular electrical coupling in the peri-infarct zone of an MHC-EGFP heart are demonstrated in *Figure 2A–H*. Similar to the example shown in *Figure 1*, voltage transients in the nonmyocytes occurred at a 1:1 ratio with the ventricular action potential during 3 Hz pacing. Shown in *Figure 2F–H* is an example wherein two neighbouring nonmyocytes electrotonically couple to the same border zone myocyte.

Properties of propagating action potential-evoked $-\Delta F/F_o$ transients recorded from border zone myocytes and juxtaposed, electrically coupled nonmyocytes are summarized in *Figure 2I* (see also Supplementary material online, *Table S1*). The median peak amplitude of ensemble averages $-\Delta F/F_o$ was by a factor of 3.5 smaller in nonmyocytes than in juxtaposed myocytes (left panel), whereas the median values for the 10%–90% rise time and 70% repolarization time of ensemble averages $-\Delta F/F_0(t)$ were respectively 4.7-fold and 3.4-fold larger in electrically coupled nonmyocytes compared with their abutting myocytes (*Figure 2I*, centre and right panel, respectively; see Supplementary material online, *Table S1*). Line-scan images series that were obtained in triplicate from infarcted MHC-EGFP hearts at 15-min intervals demonstrated stability of mean peak $-\Delta F/F_0$ amplitude and kinetics of both ventricular action potentials and nonmyocyte voltage transients over time (see Supplementary material online, *Table S2*), suggesting that differences in $-\Delta F/F_o$ transients did not arise as a consequence of electrical deterioration of the nonmyocyte.

Collectively, these results demonstrate that the electrical activity of ventricular myocytes drives cyclic electrotonic responses in coupled nonmyocytes. The mismatch between the voltage transient and the action potential waveform was not observed between juxtaposed border zone myocytes (see Supplementary material online, *Figure S3*).

3.2 Myofibroblasts contribute to the population of electrically coupled nonmyocytes in the peri-infarct zone

Based on *in vitro* studies demonstrating electrical coupling between co-cultured ventricular myocytes and cardiac myofibroblasts, we next sought to examine the possibility that myofibroblasts contribute to the population of electrically coupled nonmyocytes in the peri-infarct zone *in vivo*. Accordingly, mice carrying a periostin (Postn) promoter transgene-driving Cre recombinase (Postn-Cre)[13] were bred with a Rosa26 loxP-inactivated ZsGreen (Rosa-ZsGreen) reporter line. When these mice are crossed, any cell that expresses periostin will permanently express the recombinant green fluorescent protein ZsGreen. Our previous studies have demonstrated that both endogenous periostin as well as a the Postn-Cre transgene targets expression of a genetically encoded reporter to myofibroblasts in the injured heart.[13,14] Histological sections from Postn-Cre; Rosa-ZsGreen hearts with 1-week-old myocardial infarctions showed abundant ZsGreen-positive interstitial cells in the left ventricle within the infarct region (*Figure 3A*). ZsGreen labelled both nuclei and cytoplasm. Overlays of confocal fluorescence images on differential interference contrast images showed interstitial protrusions of $ZsGreen^+$ cells projecting along cardiomyocytes (*Figure 3A*). A 3D reconstruction of a *z*-stack of confocal fluorescence images taken from the epicardial border zone in an infarcted Postn-Cre; Rosa-ZsGreen heart revealed finger- or sheet-like projections of ZsGreen fluorescence which extended along and/or around neighbouring cardiomyocytes (*Figure 3B* and *C*).

We used immunohistochemical analyses to determine the identity of the $ZsGreen^+$ interstitial cell population. Hearts were harvested from Postn-Cre; Rosa-ZsGreen mice 1 week after myocardial infarction injury. Ten-μm thick cryosections were obtained and reacted with antibodies against vimentin or α-SMA to identify myofibroblasts.[13,15] Representative images acquired from the infarct border zone are shown in *Figure 4*. Approximately 94% of the ZsGreen-expressing cells located in the peri-infarct zone were vimentin positive (1 250 cells counted, 8 regions, and 2 hearts), while 89% were α-SMA-positive (1 490 cells counted, 8 regions, and 2 hearts). These results indicate that ZsGreen-expressing cells are myofibroblasts in the post myocardial infarction heart.

Next, we subjected infarcted Postn-Cre; Rosa-ZsGreen hearts to vital TPLSM voltage imaging to determine if ZsGreen-expressing myofibroblasts electrically couple to surrounding, ZsGreen-negative cardiomyocytes in the peri-infarct zone. Representative examples of frame-mode fluorescence images taken from the infarct border zones in dye-loaded Postn-Cre; Rosa-ZsGreen hearts are shown in the upper panels of *Figure 5A* and see Supplementary material online, *Figure S4A*. Interstitial myofibroblasts could be readily identified by virtue of their green fluorescent cytoplasm. Cardiomyocytes lacked green fluorescence and, unlike

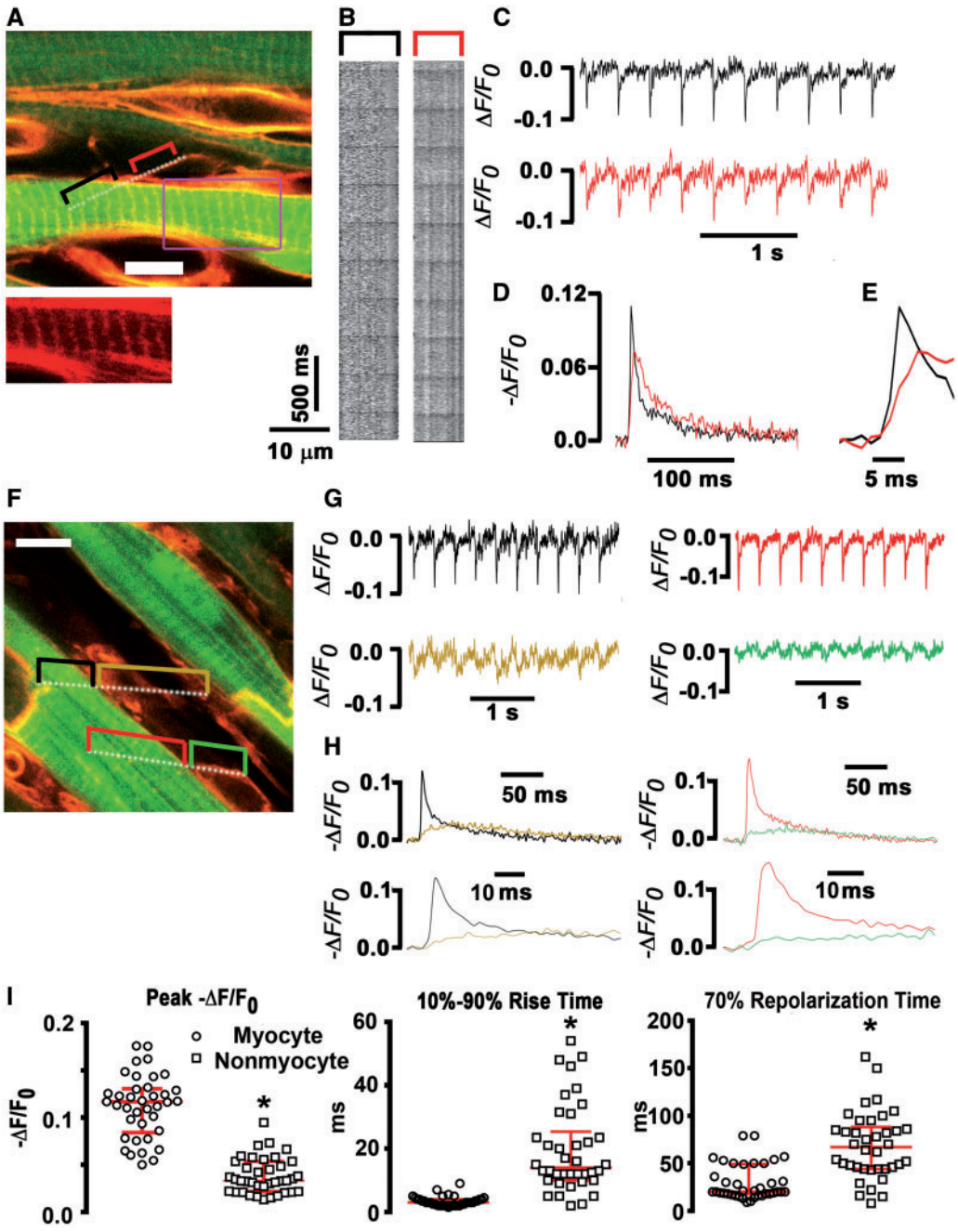

Figure 2 Ventricular myocytes electrically couple to nonmyocytes in the border zone of chronic myocardial infarction. *A*, Frame-mode fluorescence image taken from an 8-day-old infarct border zone in an ANNINE-6plus–loaded MHC-EGFP heart. EGFP marks cardiomyocytes. Dotted line indicates the position of line-scan $F(x, t)$ image acquisition. Images were acquired while the heart was electrically paced at a remote site at a frequency of 3 Hz. Lower panel is a magnified view of the red signal within the boxed region, demonstrating ANNINE-6plus staining of outer and t-tubular myocyte membranes. White scale bar 10 μm. Note the absence of ANNINE-6plus—stained membranes in some of the interstitial space compatible with the presence of collagen fibrils which do not take up the dye. *B*, Line-scan fluorescence $F(x, t)$ image for the segments of the scanning lines marked by colour-coded brackets in panels *A*. Images were normalized, filtered and the contrast increased. *C*, Line average $\Delta F/F_o(t)$ for the colour-coded segments in *A*. Traces are excerpts from line-scan recordings comprising 42 consecutive voltage transients and were filtered by a 5-point moving average. *D*, Superimposition of ensemble averages $-\Delta F/F_o(t)$ for the colour-coded segments of the scanning line in *A*. *E*, Upstrokes of myocyte and nonmyocyte $\Delta F/F_o$ transients in *D* on an expanded time scale. *F*, Frame-mode fluorescence image from 10-day-old infarct border zone in an MHC-EGFP heart. White scale bar 10 μm. *G*, Line averages $\Delta F/F_o(t)$ for the colour-coded segments in *F*. Traces are excerpts from line-scan recordings comprising 44 successive transients and were filtered by a 5-point moving average. *H*, Superimposition of ensemble averages $-\Delta F/F_o(t)$ for the correspondingly coloured segments of the scanning lines in *F*. Lower panels: upstrokes of $-\Delta F/F_o$ transients on expanded time scales. *I*, Properties of action potential-evoked $-\Delta F/F_o$ transients in border zone myocytes and juxtaposed, electrically coupled nonmyocytes. Shown are dot plots of peak amplitudes, 10%–90% rise times, and 70% repolarization times of ensemble averages $-\Delta F/F_o(t)$. The upper and lower red lines mark the first and third quartile, respectively, and the median is indicated by the centre red line. Values are from 38 coupled myocyte–nonmyocyte pairs distributed among 13 MHC-EGFP hearts with 7- to 10-day-old myocardial infarctions. *$P < 0.001$ vs. myocytes by *Wilcoxon Rank Sum* test.

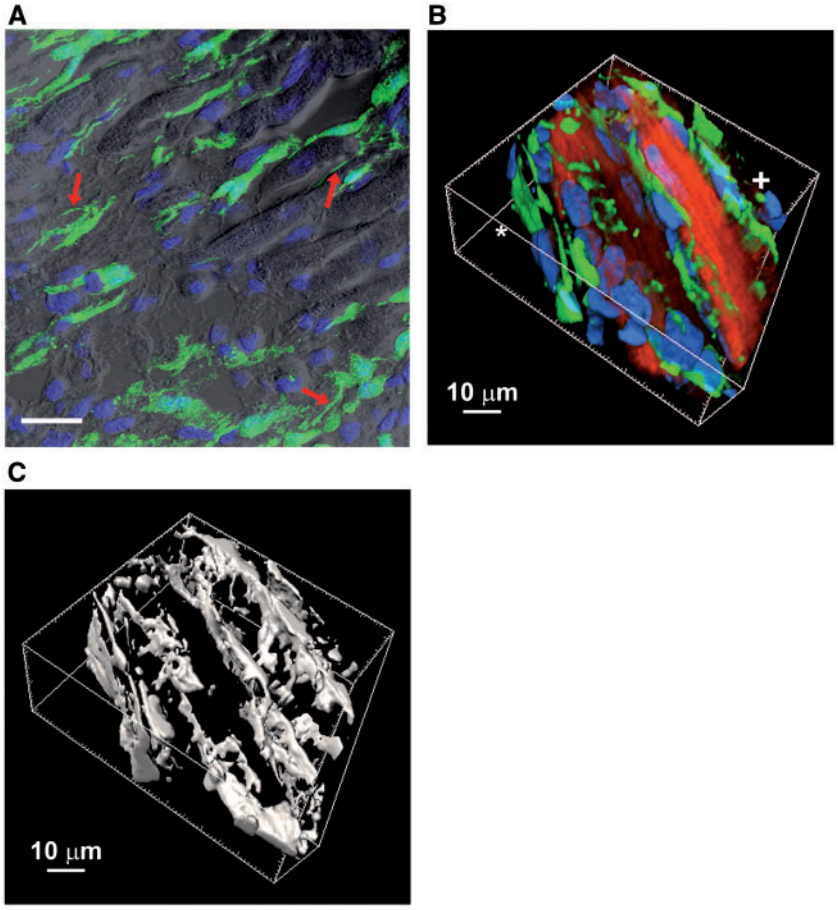

Figure 3 ZsGreen-expressing cells form a network in the infarct border zone. *A*, Representative histological section showing ZsGreen-labelled (green) interstitial cells in the infarct border zone of a Postn-Cre; ROSA-ZsGreen heart at 8 days after coronary artery ligation. Shown is a co-registration of the fluorescence confocal image and the differential interference contrast (DIC) image. Nuclei are labelled with DAPI (blue). Arrows denote extensions from ZsGreen$^+$ cells. White scale bar 20 μm. *B*, Volume rendering of the green ZsGreen fluorescence, red cardiomyocyte autofluorescence, and blue (DAPI) nuclear fluorescence. The image was reconstructed from a confocal *z*-stack acquired from a 70-μm × 70-μm × 30-μm region in the epicardial border zone of a 9-day-old infarction in a Postn-Cre; Rosa-ZsGreen heart. The asterisk and the plus sign mark the epicardial border and the infarct scar, respectively. *C*, Isosurface 3D volume rendering of the ZsGreen signal in *B*.

myofiboblasts, displayed ANNINE-6plus—stained t-tubular membranes (lower panels). The t-tubular membranes of the myocytes could exhibit an irregular pattern, indicative of their structural remodelling which is typically seen in surviving cardiomyocytes postinfarction.[16] Line-scan *F(x, t)* images revealed periodic, transient depolarizations in the myofibroblast membranes occurring in phase with those in the juxtaposed cardiomyocyte membranes (*Figure 5B* and see Supplementary material online, *Figure S4B*), suggesting that they were entrained. Averaged $\Delta F/F_0(t)$ traces which were generated from the line-scan data for the cardiomyocytes and myofibroblasts confirmed that fluctuations in transmembrane potential in the latter occurred concomitantly with the action potentials in the juxtaposed myocytes in a 1:1 ratio (*Figure 5C* and see Supplementary material online, *Figure S4C*), indicating that myofibroblasts electrotonically couple to border zone myocytes. Superimposition of ensemble averages $\Delta F/F_0(t)$ (*Figure 5D* and *E* and see Supplementary material online, *Figure S4D* and *E*) demonstrated smaller peak $\Delta F/F_0$ as well as slower rates of de- and repolarization of the electrotonic transients in the myofibroblasts compared with those in the abutting myocyte. On average, the peak amplitude and kinetics of myofibroblast voltage transients in infarcted Postn-Cre; Rosa-ZsGreen hearts were indistinguishable from those of electrically coupled nonmyocytes in infarcted MHC-EGFP hearts (*Figure 5F* and see Supplementary material online, *Table S1*). Overall, these results indicate that myofibroblasts contribute to the population of electrically coupled nonmyocytes in the chronically infarcted heart.

3.3 Presence of connexins at myocyte–myofibroblast junctions in the infarct border zone

In vitro studies have demonstrated that gap junctions composed of connexin43 (Cx43) or connexin45 (Cx45) mediate direct electrical coupling between heterocellular pairs formed by cardiac myofibroblasts and co-cultured ventricular myocytes.[2] Fibroblasts accumulating in the border zone of chronic infarcts have been shown to express Cx43 and/or Cx45.[17] Accordingly, we used immunohistochemistry to examine

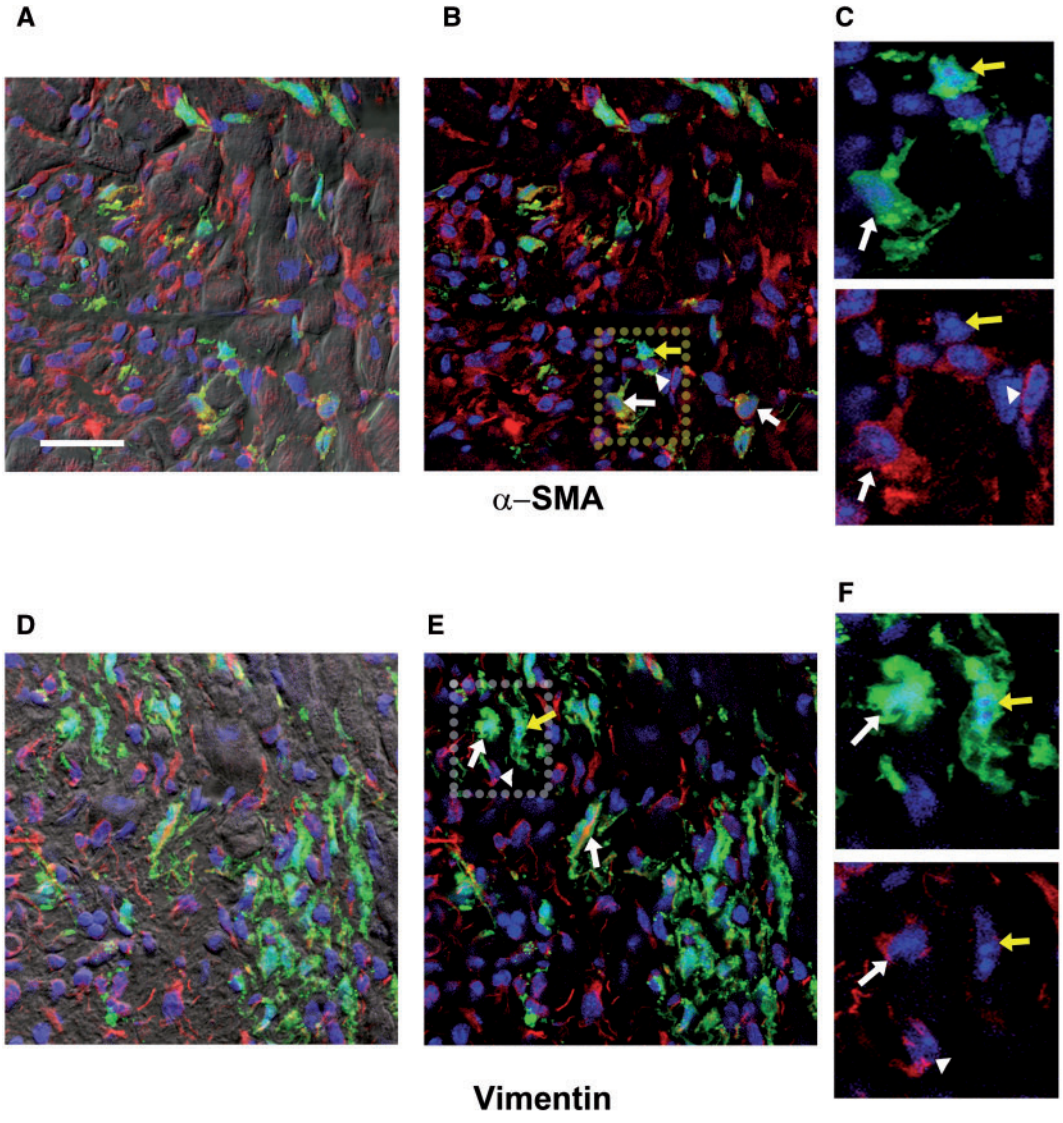

Figure 4 ZsGreen-expressing cells in the infarct border zone of Postn-Cre; ROSA-ZsGreen hearts are myofibroblasts. *A–F*, Representative immunohistochemical images demonstrating staining of ZsGreen-positive cells for α-SMA (*A–C*) or vimentin (*D–F*) in the infarct border zone of Postn-Cre; ROSA-ZsGreen hearts at 8 days after coronary artery ligation. Panels *A* and *D* show confocal fluorescence images (green: ZsGreen, red: vimentin or α-SMA, blue: nuclei) overlaid on DIC images, middle panels show confocal fluorescence images only. Panels *C* and *F* are magnified views of the boxed regions (dotted lines) in the panels *B* and *E*. White arrows demark vimentin (α-SMA) and ZsGreen co-labelling, yellow arrows show ZsGreen labelling only, and the white arrow heads show vimentin (α-SMA) expression only without ZsGreen. White scale bar 20 μm.

whether the same connexin types can be found at myocyte–myofibroblast contacts *in vivo*. Tissue sections from infarcted MHC-EGFP hearts were reacted with antibodies against α-smooth muscle actin and Cx43 or Cx45, and subjected to confocal microscopy to visualize connexin expression and distribution. Representative 3D reconstructions of confocal fluorescence images obtained from the infarct border zone as well as from a zone remote from the infarct are shown in *Figure 6*. Cx43 was organized in the typical intercalated disk pattern between paired adjoining cardiomyocytes in viable ventricular tissue remote from the peri-infarct zone (*Figure 6A*). In sharp contrast, sparse, punctate-type labelling for Cx43 (*Figure 6B* and see Supplementary material online, *Figure S5*) or Cx45 (*Figure 6C* and see Supplementary material online, *Figure S5*) was observed in some regions of abutment of EGFP-positive myocytes and α-SMA-expressing myofibroblasts. The volume of the junctional connexin was determined by generating isosurfaces of the connexin immunosignal distributed along cell-to-cell contacts in confocal z-stacks and normalized to the cell-to-cell contact area to estimate the density of junctional connexin expression (see Supplementary material online, *Movie S1*). These analyses revealed a significantly lower Cx43 density in myocyte–myofibroblast contact regions compared to the intercalated disc region between adjoined cardiomyocytes (left and middle panel *Figure 6D*). On the other hand, Cx43 density markedly exceeded Cx45 density at heterocellular junctions (middle and right panel *Figure 6D*). Additional immunohistochemical studies in tissue sections from infarcted Postn-Cre; Rosa-ZsGreen hearts confirmed the presence of both anti-Cx43 and anti-Cx45 immunoreactivity at junctions between

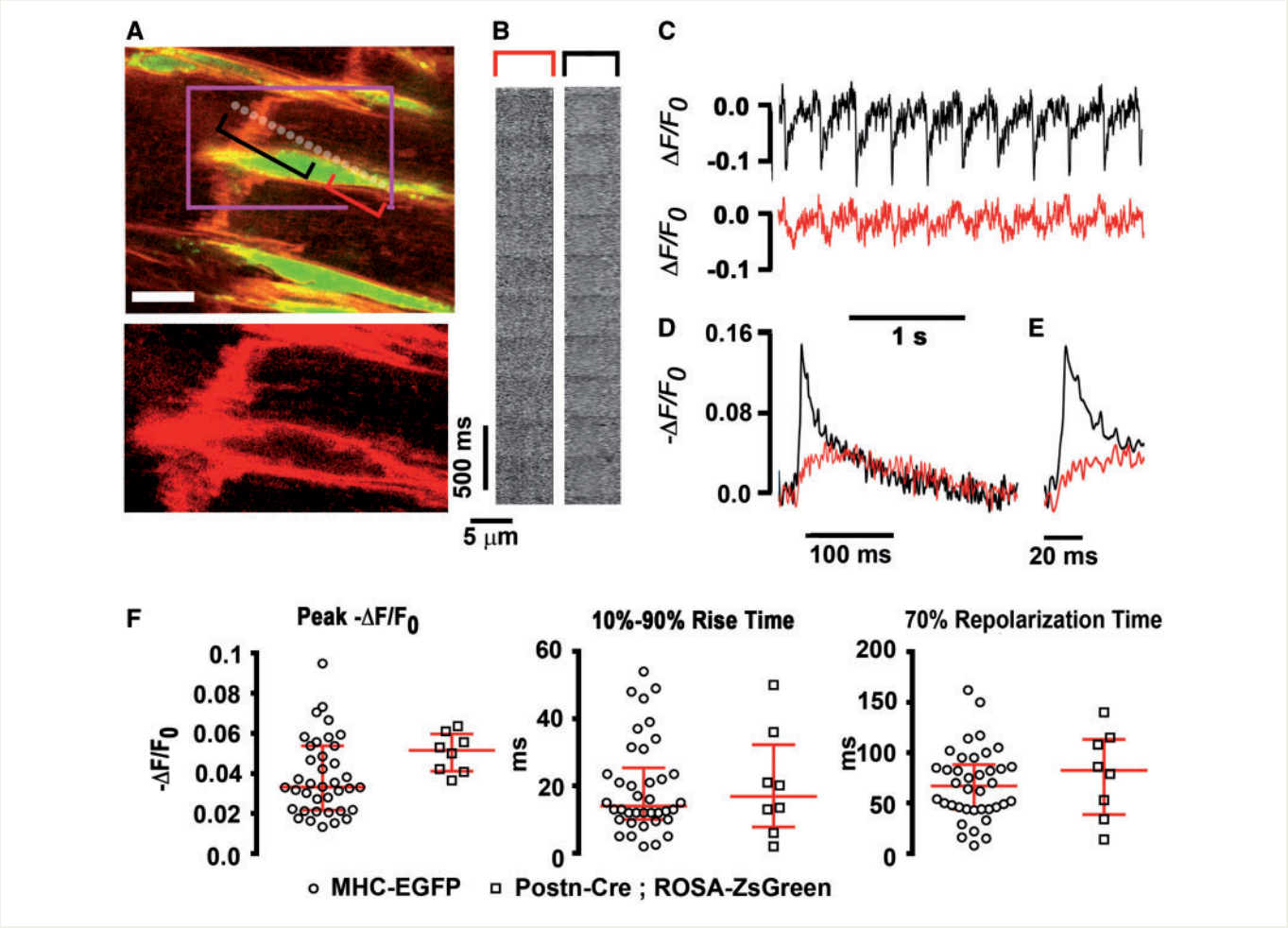

Figure 5 Cardiomyocytes electrically couple to myofibroblasts in the border zone of chronic myocardial infarction. *A*, Frame-mode fluorescence image taken from a 10-day old infarct border zone in an ANNINE-6plus—loaded Postn-Cre; ROSA-ZsGreen heart. EGFP marks myofibroblasts. Dotted line demarks the position of line-scan *F(x, t)* image acquisition. Lower panel is a magnified view of the red signal within the boxed region. White scale bar 10 μm. *B*, Line-scan fluorescence *F(x, t)* image for the segments of the scanning lines marked by the correspondingly coloured brackets in *A*. Images were normalized, filtered and the contrast increased. *C*, Line average $\Delta F/F_o(t)$ for the colour-coded segments in *A*. Traces are excerpts from a line-scan recording comprising 22 consecutive voltage transients and were filtered by a 5-point moving average. *D*, Superimposition of ensemble averages $-\Delta F/F_o(t)$ for the colour-coded segments of the scanning line in *A*. *E*, Upstrokes of myocyte and nonmyocyte $\Delta F/F_o$ transients in *D* on an expanded time scale. *F*, Comparison of action potential-evoked $-\Delta F/F_o$ transients recorded from ZsGreen—expressing cells and non-expressing cells in the infarct border zones of Postn-Cre; ROSA-ZsGreen and MHC-EGFP hearts, respectively. Dot plots from 38 and 8 coupled nonmyocytes distributed among 13 MHC-EGFP hearts and 3 Postn-Cre; ROSA-ZsGreen hearts, respectively, with 7- to 10-day-old myocardial infarctions. Upper and lower red lines indicate first and third interquartiles, respectively, while the centre red lines mark the medians. No statistically significant differences were detected between the two groups by *t*-test (peak $-\Delta F/F_o$ and 70% Repolarization Time) or *Mann–Whitney U*-test ($P > 0.05$).

myofibroblasts and juxtaposed cardiomyocytes (see Supplementary material online, *Figure S6*). Notably, we also found connexin immunostaining alongside contacts between digit-like, interstitial extensions of myofibroblasts and juxtaposed cardiomyocytes (see Supplementary material online, *Figure S6*).

4. Discussion

Using two independent reporter mouse lines, we provide direct evidence, on a cellular scale in the living heart, that ventricular myocytes electrotonically communicate with juxtaposed myofibroblasts in the border zone of chronic myocardial infarction, giving rise to periodic voltage transients of the myofibroblast membranes occurring in phase with the action potential of the coupled myocyte. The electrotonic responses in the myofibroblasts exhibited slower rates of de- and repolarization compared to the action potential waveform of the myocytes, suggesting low-pass filtering of the transmitted original voltage signal. The presence of connexins at heterocellular junctions, albeit at low density, supports a role of gap junctions in establishing myofibroblast–myocyte electrical coupling.

4.1 Cell type contributing to and possible mechanisms responsible for heterocellular electrical coupling in the infarct border zone

Our immunohistochemical analyses indicate that the periostin promoter transgene driving-Cre targets ZsGreen expression to myofibroblasts in

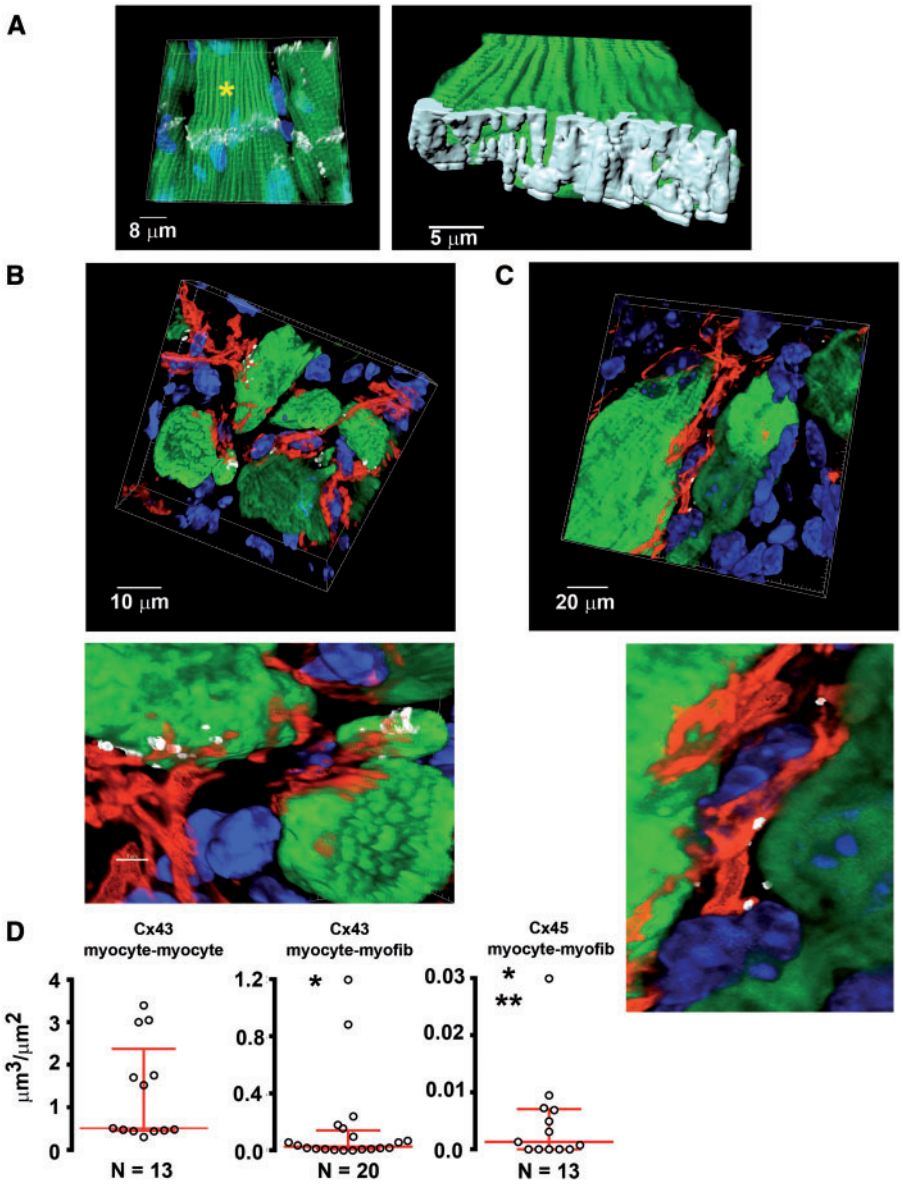

Figure 6 Connexin expression at myocyte–myocyte and myocyte–myofibroblast junctions. *A*, Left panel shows 3D reconstruction of fluorescence confocal images obtained from the end-to-end intercalated disc regions between paired ventricular cardiomyocytes in the remote, uninjured myocardium of an MHC-EGFP heart stained for Cx43. White indicates Cx43; green, EGFP; blue, DAPI. Right panel shows the isosurface 3D volume rendering of the junctional Cx43 immunosignal in the left panel overlaid on a 3D reconstruction of the EGFP signal in the cardiomyocyte marked with an asterisk in *A*. *B* and *C*, Left panels: 3D reconstructions of fluorescence confocal images that were acquired from the infarct border zones in MHC-EGFP hearts at 9 days following coronary artery ligation. Sections were stained for α-SMA (red) and Cx43 or Cx45 (*B* and *C*, respectively; white). Green indicates EGFP; blue, DAPI. The white signals represent the isosurface volume renderings of the connexin immunereactivity at the myocyte–myofibroblast junctions. Right panels are magnified views of sub-regions in the 3D renderings shown in the left panels. *D*, Connexin densities at myocyte–myocyte and myocyte–myofibroblast junctions in the border zone of chronic myocardial infarction. Dot plots of connexin density with first and third interquartiles marked by the upper and lower red lines, respectively, and the median shown as centre red lines. *N* indicates the number of myocytes. Data were obtained from three injured MHC-EGFP hearts for Cx43 at myocyte–myocyte junctions (left panel; median [25%–75% interquartiles]: 0.51 [0.45–2.37] $\mu m^3/\mu m^2$), and for Cx43 and Cx45 at myocyte–myofibroblast (myofib) junctions [Cx43, middle panel: 0.027 [0.009–0.140] $\mu m^3/\mu m^2$; Cx45, right panel: 0.0013 [0.000–0.0071 $\mu m^3/\mu m^2$) with 1–2 regions each quantified. *$P < 0.005$ vs. Cx43 density at myocyte–myocyte junctions; **$P = 0.023$ vs. Cx43 density at myocyte–myofibroblast junctions. *Kruskal–Wallis One-Way ANOVA on Ranks* followed by *Dunn's* test for *post hoc* multiple comparisons.

Postn-Cre; Rosa-ZsGreen hearts with myocardial infarction injury, in agreement with our previous observations demonstrating fibroblast-restricted expression of a beta-galactosidase reporter in hearts from Postn-Cre; Rosa-lacZ mice following pressure overload-induced injury.[13]

Our findings are also in agreement with those reported by Kanisicak *et al.* who demonstrated myofibroblast-specific EGFP expression in ischemically injured hearts from crosses of Rosa-eGFP mice with mice carrying a regulatable Cre recombinase cassette knocked into the *Postn*

gene locus.[15] Overall, these observations support the notion that electrically coupled, ZsGreen$^+$ cells in infarcted Postn-Cre; Rosa-ZsGreen hearts are myofibroblasts. It is not possible to determine with certainty what cell type(s) underlie(s) the population of electrically coupled nonmyocytes in infarcted MHC-EGFP hearts. However, the striking similarity between their voltage transient properties and those of coupled ZsGreen$^+$ cells combined with the presence of anti-connexin immunoreactivity at the junction between EGFP$^+$ cardiomyocytes and α-SMA-expressing cells strongly suggest that myofibroblasts significantly contribute to the population of electrically coupled nonmyocytes in infarcted MHC-EGFP hearts.

Two recent studies have provided independent evidence for the existence of myocyte–nonmyocyte electrical coupling in the fibrotically remodelled ventricular myocardium. Quinn and coworkers used transgenic mice in which the Wilms-tumor-suppressor-1 promoter targets expression of a FRET-based, genetically encoded voltage sensor to nonmyocytes, including cardiac myofibroblasts.[7] Epifluorescence measurements from small (600 × 600 μm^2) regions distributed across the left ventricular epicardial surface of isolated perfused hearts of cryoinjured, transgenic mice revealed rhythmic, cardiomyocyte action potential-like electrical activity at the scar border tissue, compatible with electrotonic signal transmission from myocytes to nonmyocytes.[7] Using an identical injury model, Mahoney *et al.* demonstrated reciprocal electrotonic conduction between the scar and uninjured myocardium through optical voltage mapping.[6] Our study provides additional, independent evidence for the existence of myofibroblast–myocyte electrical coupling in the fibrotically remodelled heart, using a myocardial infarction injury model. Furthermore, the use of TPLSM-based, micron-scale voltage monitoring in conjunction with targeted expression of fluorescent reporters enables precise correlation of cell type and electrical function *in situ*, providing critical information on the electrical activity of individual, electrically coupled myofibroblasts across the border zone tissue.

Our immunohistochemical analyses revealed low expression of both Cx43 and Cx45 in contact regions between paired myofibroblasts and myocytes, in agreement with previous studies reporting similarly low expression of these connexin types in the infarct border zone of sheep hearts.[17] These findings suggest a possible role of gap junctions in establishing heterocellular electrotonic communication in the present study, as has been well documented in experimental systems consisting of neonatal ventricular myocytes and cardiac (myo)fibroblasts.[2] In a more recent study, Mahoney *et al.* demonstrated that scar–muscle electrical coupling was significantly reduced in cryoinjured hearts from fibroblast-specific protein-1 driven conditional Cx43 knock-out mice, providing strong, direct evidence for a role of Cx43 gap junctions in supporting heterocellular electrical coupling in fibrotically remodelled hearts *in vivo*.[6] Whether connexin gap junctions similarly contribute to heterocellular coupling in the border zone of healing myocardial infarctions as observed in the present study remains to be shown.

Other, gap junction-independent, mechanisms have previously been implicated in the establishment of heterocellular electrical coupling, including the formation of tunnelling nanotubes, mechanosensitive feedback, and ephaptic transmission.[7,18–20] Nanotubes have been shown to enable transfer of GFP between different cell types.[21] Epifluorescence analyses of infarct border zones in MHC-EGFP and Postn-Cre; Rosa-ZsGreen hearts revealed that green fluorescence was restricted to cardiomyocytes or myofibroblasts, respectively. This was confirmed by vital TPLSM imaging which demonstrated the existence of electrically connected, EGFP negative nonmyocytes in MHC-EGFP hearts as well as ZsGreen-negative cardiomyocytes in Postn-Cre; Rosa-ZsGreen hearts, arguing against nanotubular communication as a means of heterocellular coupling under the experimental conditions studied here. Because treatment with blebbistatin and ryanodine effectively eliminated cardiomyocyte contraction during *in situ* imaging, mechanical stretch relayed across heterocellular junctions is unlikely to be responsible for activating adjacent myofibroblasts by electromechanical feedback. The possibility that electrical field, i.e. ephaptic, transmission contributes to myofibroblast–myocyte coupling cannot be ruled out.[20] To date, simulation studies examining the possibility of field effect transmission between excitable and nonexcitable cells have not been published.

4.2 Low-pass filtering of the nonmyocyte voltage response

Myofibroblast voltage transients exhibited lower peak amplitudes as well as slower rates of de- and repolarization compared to the action potentials recorded from juxtaposed myocytes. Because we have not calibrated the optical voltage signal by using reference signals of known magnitude, it is not possible to quantitatively compare the amplitude of the nonmyocyte voltage response to that of the cardiomyocyte action potential. On the other hand, disparities between myocytes and nonmyocytes in the kinetics of their respective voltage transients should remain unaffected by cell type-dependent differences in the dye's voltage sensitivity. Mahoney and co-workers used conventional microelectrode recordings to compare electrical signals recorded from scar tissue of cryoinjured mouse hearts with action potentials obtained from remote, uninjured myocardium.[6] Voltage transients from the scar on average exhibited slower rates of de- and repolarization, in striking similarity to our optical recordings from single border zone myofibroblasts. Several mechanisms acting individually or synergistically can give rise to these filtered voltage responses in myofibroblasts, including (i) low levels of electrical coupling between myocytes and myofibroblasts, (ii) low myofibroblast membrane resistance, (iii) capacitive loading effects, and (iv) presence of time- and/or voltage-dependent conductances in the myofibroblast membranes. Our immunohistochemical analyses demonstrate a markedly reduced (ca. 20-fold) Cx43 density at the myofibroblast-myocyte contact zones compared to that observed in the intercalated disc regions between paired cardiomyocytes in the uninjured myocardium. Assuming a major role for Cx43 gap junctions in establishing heterocellular coupling and further assuming proportionality between transjunctional conductance and Cx43 density,[22] one would expect such low connexin levels to markedly attenuate the electrotonic transmission to the myofibroblasts. Indeed, computational analyses have documented that the profile of simulated voltage responses in the (myo)fibroblast at reduced coupling conductances closely resembles that of membrane potential waveforms recorded from *in situ* myofibroblasts in the present study.[4,5,23] However, extrapolating the degree of gap junctional coupling from immmunohistochemical data is problematic because this approach fails to detect non-clustered connexins in small contact areas,[22] underestimating transjunctional conductance.

Second, a low input resistance (relative to the junctional resistance) of the coupled myofibroblast could contribute to the attenuation of the transmitted voltage response. Previous measurements found an apparent input resistance of between ∼6 and ∼11 GΩ in isolated rat ventricular fibroblasts.[24,25] However, corresponding measurements in cardiac myofibroblasts are lacking, making it impossible to estimate the impact of myofibroblast input resistance on the shape of the electrotonic response.

Third, the mismatch between the waveform of the myocyte action potential and that of the membrane potential changes in the coupled

myofibroblast could result from a large surface membrane area of the latter relative to that of a myocyte, giving rise to capacitive loading effects that ultimately determine the extent of changes in membrane potential excursion in the nonmyocyte. Computer simulations by MacCannell *et al.* have demonstrated that increasing the ratio of the fibroblast/myocyte membrane capacitance slowed kinetics of the electrotonic responses in the fibroblast, similar to what was observed in nonmyocytes here.[5]

Fourth, other computational analyses have suggested that the interplay of low intercellular conductance and activation of time- and voltage-dependent ionic currents in the coupled myofibroblasts can give rise to pronounced phase shifts between the myocyte and myofibroblast voltage responses such as those seen in the *in situ* myocardium.[4]

Although we previously reported hour-long stability of the dye responses for *in situ* cardiomyocytes,[8] the somewhat blurred ANNINE-6plus fluorescence in myofibroblasts (see for example *Figures 2F* and *5A*) suggests dye leakage into the cytoplasm and subsequent uptake by non-plasmalemmal membranes (e.g. mitochondria). However, we think it more likely that the 'blur' reflects portions of the outer membranes of myofibroblasts which are aligned parallel to the focal plane of the 2-photon imaging system.

Our results obtained in infarcted MHC-EGFP hearts document that the properties of nonmyocyte voltage transients are indistinguishable from those recorded in membranes of $ZsGreen^{+}$ cells, i.e. myofibroblasts, in injured Postn-Cre; Rosa-ZsGreen hearts, suggesting that contamination from other non-excitable interstitial cells (e.g. endothelial cells) to the fluorescence signal is negligible.

Previous studies have demonstrated that atrial myofibroblasts in culture express *SCN5a*, the gene encoding for the pore forming subunit of the cardiac voltage-gated sodium channel.[26] Whether cardiac voltage-gated sodium current contributes to the generation of depolarizing transients in border zone myofibroblasts remains to be determined.

4.3 Functional consequences of heterocellular coupling

Differences in magnitude and time course of changes in transmembrane voltage between the coupled myofibroblast and myocyte during the course of a ventricular action potential give rise to electrotonic currents across the heterocellular junction, influencing excitability, refractoriness, automaticity, and conduction of the border zone myocardium.[2,3,27,28]

Coupled myofibroblasts would also impose a capacitive load on border zone cardiomyocytes through contributing additional membrane area to be charged and discharged by cardiomyocytes, effectively diminishing cardiomyocyte channel density. This in turn may significantly alter cardiomyocyte membrane potential, such as action potential generation and/or duration.

Heterocellular coupling-induced changes in the myocyte action potential waveform would be predicted to alter $[Ca^{2+}]_i$ transient properties in the myocyte, via modulation of membrane potential-regulated calcium transport pathways, and thus affect myocardial inotropy. *Vice versa*, Ca^{2+} ions flowing from myocytes to myofibroblasts through open gap junctions as well as repetitive electrotonic depolarizations occurring in the myofibroblast in response to each myocyte action potential, may regulate $[Ca^{2+}]_i$ homeostasis and thus, excitation–secretion coupling, resulting in the release of paracrine and/or autocrine factors.

4.4 Limitations and perspectives

The fluorescence-based technique used here is suitable to monitor changes in membrane voltage, but it does not allow measurements of the absolute membrane potential. It is therefore not possible to assess the extent to which myofibroblast–myocyte coupling controls the resting membrane potential of either cell. Although calculations of $\Delta F/F_o$ use 0 as baseline for both myocytes and myofibroblasts, this does not imply that the resting membrane potentials are equal in the two cell types. Further, our approach does not provide quantitative estimates of the prevalence of heterocellular coupling events in the infarct border zone. Alternative experimental approaches are warranted to address these important aspects of nonmyocyte–myocyte interactions.

Supplementary material

Supplementary material is available at *Cardiovascular Research* online.

Acknowledgements

We acknowledge the help of Paige Snider in generating and genotyping the Postn-Cre; Rosa-ZsGreen reporter mice. We further acknowledge the assistance of Maria M. Kamocka (Indiana Centre for Biological Microscopy) with 3D image processing.

Conflict of interest: none declared.

Funding

This work was supported by a National Institutes of Health grant (RO1HL075165 to M.R., RO1HL60714 to S.J.C.), the Riley Children's Foundation, and by the Indiana University School of Medicine Strategic Research Initiative.

References

1. de Jong S, van Veen TAB, van Rijen HVM, de Bakker JMT. Fibrosis and cardiac arrhythmias. *J Cardiovasc Pharm* 2011;**57**:630–638.
2. Gaudesius G, Miragoli M, Thomas SP, Rohr S. Coupling of cardiac electrical activity over extended distances by fibroblasts of cardiac origin. *Circ Res* 2003;**93**:421–428.
3. Miragoli M, Gaudesius G, Rohr S. Electrotonic modulation of cardiac impulse conduction by myofibroblasts. *Circ Res* 2006;**98**:801–810.
4. Jacquemet V, Henriquez CS. Modelling cardiac fibroblasts: interactions with myocytes and their impact on impulse propagation. *Europace* 2007;**9**:vi29–vi37.
5. MacCannell KA, Bazzazi H, Chilton L, Shibukawa Y, Clark RB, Giles WR. A mathematical model of electrotonic interactions between ventricular myocytes and fibroblasts. *Biophys J* 2007;**92**:4121–4132.
6. Mahoney VM, Mezzano V, Mirams GR, Maass K, Li Z, Cerrone M, Vasquez C, Bapat A, Delmar M, Morley GE. Connexin43 contributes to electrotonic conduction across scar tissue in the intact heart. *Sci Rep* 2016;**6**:26744.
7. Quinn TA, Camelliti P, Rog-Zielinska EA, Siedlecka U, Poggioli T, O'toole ET, Knöpfel T, Kohl P. Electrotonic coupling of excitable and nonexcitable cells in the heart revealed by optogenetics. *Proc Natl Acad Sci USA* 2016;**113**:14852–14857.
8. Bu G, Adams H, Berbari EJ, Rubart M. Uniform action potential repolarization within the sarcolemma of in situ ventricular cardiomyocytes. *Biophys J* 2009;**96**:2532–2546.
9. Murry CE, Soonpaa MH, Reinecke H, Nakajima H, Nakajima HO, Rubart M, Pasumarthi KB, Virag JI, Bartelmez SH, Poppa V, Bradford G, Dowell JD, Williams DA, Field LJ. Haematopoietic stem cells do not transdifferentiate into cardiac myocytes in myocardial infarcts. *Nature* 2004;**428**:664–668.
10. Freeman K, Tao W, Sun H, Soonpaa MH, Rubart M. In situ three-dimensional reconstruction of mouse heart sympathetic innervation by two-photon excitation fluorescence imaging. *J Neurosci Methods* 2014;**221**:48–61.
11. Rubart M, Pasumarthi KB, Nakajima H, Soonpaa MH, Nakajima HO, Field LJ. Physiological coupling of donor and host cardiomyocytes after cellular transplantation. *Circ Res* 2003;**92**:1217–1224.
12. Young PA, Clendenon SG, Byars JM, Decca RS, Dunn KW. The effects of spherical aberration on multiphoton fluorescence excitation microscopy. *J Microsc* 2011;**242**:157–165.
13. Takeda N, Manabe I, Uchino Y, Eguchi K, Matsumoto S, Nishimura S, Shindo T, Sano M, Otsu K, Snider P, Conway SJ, Nagai R. Cardiac fibroblasts are essential for the adaptive response of the murine heart to pressure overload. *J Clin Invest* 2010;**120**:254–265.
14. Snider P, Standley KN, Wang J, Azhar M, Doetschman T, Conway SJ. Origin of cardiac fibroblasts and the role of periostin. *Circ Res* 2009;**105**:934–947.

15. Kanisicak O, Khalil H, Ivey MJ, Karch J, Maliken BD, Correll RN, Brody MJ, J Lin SC, Aronow BJ, Tallquist MD, Molkentin JD. Genetic lineage tracing defines myofibroblast origin and function in the injured heart. *Nat Commun* 2016;**7**:12260.
16. Louch WE, Mørk HK, Sexton J, Strømme TA, Laake P, Sjaastad I, Sejersted OM. T-tubule disorganization and reduced synchrony of Ca2+ release in murine cardiomyocytes following myocardial infarction. *J Physiol (Lond)* 2006;**574**:519–533.
17. Camelliti P, Devlin GP, Matthews KG, Kohl P, Green CR. Spatially and temporally distinct expression of fibroblast connexins after sheep ventricular infarction. *Cardiovasc Res* 2004;**62**:415–425.
18. He K, Shi X, Zhang X, Dang S, Ma X, Liu F, Xu M, Lv Z, Han D, Fang X, Zhang Y. Long-distance intercellular connectivity between cardiomyocytes and cardiofibroblasts mediated by membrane nanotubes. *Cardiovasc Res* 2011;**92**:39–47.
19. Thompson SA, Copeland CR, Reich DH, Tung L. Mechanical coupling between myofibroblasts and cardiomyocytes slows electric conduction in fibrotic cell monolayers. *Circulation* 2011;**123**:2083–2093.
20. Mori Y, Fishman GI, Peskin CS. Ephaptic conduction in a cardiac strand model with 3D electrodiffusion. *Proc Natl Acad Sci USA* 2008;**105**:6463–6468.
21. Koyanagi M, Brandes RP, Haendeler J, Zeiher AM, Dimmeler S. Cell-to-cell connection of endothelial progenitor cells with cardiac myocytes by nanotubes: a novel mechanism for cell fate changes?. *Circ Res* 2005;**96**:1039–1041.
22. McCain ML, Desplantez T, Geisse NA, Rothen-Rutishauser B, Oberer H, Parker KK, Kleber AG. Cell-to-cell coupling in engineered pairs of rat ventricular cardiomyocytes: relation between Cx43 immunofluorescence and intercellular electrical conductance. *Am J Physiol Heart Circ Physiol* 2012;**302**:H443–H450.
23. Maleckar MM, Greenstein JL, Giles WR, Trayanova NA. Electrotonic coupling between human atrial myocytes and fibroblasts alters myocyte excitability and repolarization. *Biophys J* 2009;**97**:2179–2190.
24. Shibukawa Y, Chilton EL, Maccannell KA, Clark RB, Giles WR. K+ currents activated by depolarization in cardiac fibroblasts. *Biophys J* 2005;**88**:3924–3935.
25. Chilton L, Ohya S, Freed D, George E, Drobic V, Shibukawa Y, Maccannell KA, Imaizumi Y, Clark RB, Dixon IM, Giles WR. K+ currents regulate the resting membrane potential, proliferation, and contractile responses in ventricular fibroblasts and myofibroblasts. *Am J Physiol Heart Circ Physiol* 2005;**288**:H2931–H2939.
26. Chatelier S, Mercier A, Tremblier B, Thériault O, Moubarak M, Benamer N, Corbi P, Bois P, Chahine M, Faivre JF. A distinct *de novo* expression of $Na_v1.5$ sodium channels in human atrial fibroblasts differentiated into myofibroblasts. *J Physiol* 2012;**590**:4307–4319.
27. Askar SF, Bingen BO, Swildens J, Ypey DL, van der Laarse A, Atsma DE, Zeppenfeld K, Schalij MJ, de Vries AA, Pijnappels DA. Connexin43 silencing in myofibroblasts prevents arrhythmias in myocardial cultures: role of maximal diastolic potential. *Cardiovasc Res* 2012;**93**:434–444.
28. Vasquez C, Mohandas P, Louie KL, Benamer N, Bapat AC, Morley GE. Enhanced fibroblast–myocyte interactions in response to cardiac injury. *Circ Res* 2010;**107**:1011–1020.